JOURNAL OF PHYSIOLOGY AND PHARMACOLOGY 2018, 69, 1, 99-107
www.jpp.krakow.pl | DOI: 10.26402/jpp.2018.1.11

B. HORVATH[1,2], N. SZENTANDRASSY[1,3], R. VERESS[1], D. BARANYAI[1], K. KISTAMAS[1], J. ALMASSY[1], A. TOTH[4], J. MAGYAR[1,5], T. BANYASZ[1], P.P. NANASI[1,3]

EFFECT OF THE INTRACELLULAR CALCIUM CONCENTRATION CHELATOR BAPTA ACETOXY-METHYLESTER ON ACTION POTENTIAL DURATION IN CANINE VENTRICULAR MYOCYTES

[1]Department of Physiology, Faculty of Medicine, University of Debrecen, Debrecen, Hungary;
[2]Faculty of Pharmacy, University of Debrecen, Debrecen, Hungary;
[3]Department of Dental Physiology and Pharmacology, Faculty of Dentistry, University of Debrecen, Debrecen, Hungary;
[4]Department of Pharmacology and Pharmacotherapy, Faculty of Medicine, University of Szeged, Szeged, Hungary;
[5]Division of Sport Physiology, Department of Physiology, Faculty of Medicine, University of Debrecen, Debrecen, Hungary

Intracellular calcium concentration ($[Ca^{2+}]_i$) is often buffered by using the cell-permeant acetoxy-methylester form of the Ca^{2+} chelator BAPTA (BAPTA-AM) under experimental conditions. This study was designed to investigate the time-dependent actions of extracellularly applied BAPTA-AM on action potential duration (APD) in cardiac cells. Action potentials were recorded from enzymatically isolated canine ventricular myocytes with conventional sharp microelectrodes. The effect of BAPTA-AM on the rapid delayed rectifier K^+ current (I_{Kr}) was studied using conventional voltage clamp and action potential voltage clamp techniques. APD was lengthened by 5 μM BAPTA-AM - but not by BAPTA - and shortened by the Ca^{2+} ionophore A23187 in a time-dependent manner. The APD-lengthening effect of BAPTA-AM was strongly suppressed in the presence of nisoldipine, and enhanced in the presence of BAY K8644, suggesting that a shift in the $[Ca^{2+}]_i$-dependent inactivation of L-type Ca^{2+} current may be an important underlying mechanism. However, in the presence of the I_{Kr}-blocker dofetilide or E-4031 APD was shortened rather than lengthened by BAPTA-AM. Similarly, the APD-lengthening effect of 100 nM dofetilide was halved by the pretreatment with BAPTA-AM. In line with these results, I_{Kr} was significantly reduced by extracellularly applied BAPTA-AM under both conventional voltage clamp and action potential voltage clamp conditions. This inhibition of I_{Kr} was partially reversible and was not related to the Ca^{2+} chelator effect BAPTA-AM. The possible mechanisms involved in the APD-modifying effects of BAPTA-AM are discussed. It is concluded that BAPTA-AM has to be applied carefully to control $[Ca^{2+}]_i$ in whole cell systems because of its direct inhibitory action on I_{Kr}.

Key words: *calcium chelators, intracellular calcium concentration, action potential duration, cardiac ion currents, potassium ion, currents, ventricular myocytes*

INTRODUCTION

In cellular electrophysiological studies intracellular calcium concentration is often buffered under experimental conditions because of the wide variety of Ca^{2+}-dependent ion currents, including Na^+ (1, 2), Ca^{2+} (3, 4), K^+ (5, 6), Cl^- (7, 8), Na^+-Ca^{2+} exchanger (9, 10) and nonspecific cation (11, 12) currents in the heart. In voltage clamp experiments, using typically patch pipettes with large pore diameters, buffering of $[Ca^{2+}]_i$ is relatively easy, since dialysis of the intracellular compartment with the Ca^{2+} chelator BAPTA is readily performed by the pipette solution. When action potentials are recorded under physiological conditions with conventional sharp microelectrodes this approach is not available due to the small tip diameter of the recording electrode. In this case the cell-permeant acetoxy-methylester form of a Ca^{2+} chelator can be applied to reduce $[Ca^{2+}]_i$. Such experiments have been performed for decades and their results were interpreted exclusively in terms of buffering $[Ca^{2+}]_i$ (13-17) - in spite of the fact that BAPTA-AM (and also EGTA-AM) has been shown to interact with K^+ channels expressed in HEK cells (18). Since drug-channel interactions may be markedly different in native and expressed ion channels (19), it was reasonable to test the effect of BAPTA-AM on I_{Kr}, which current has the greatest influence on ventricular repolarization in larger mammals. For the same reason the effect of BAPTA-AM on action potential morphology was also studied. Canine ventricular cells were chosen in these experiments because the electrophysiological properties of this preparation best resemble those of human myocardium (20, 21).

Our results indicate that in mammalian ventricular cardiomyocytes BAPTA-AM affects APD in two separate ways: in addition to the consequences of $[Ca^{2+}]_i$ buffering, and thus modifying the activity of Ca^{2+}-dependent ionic currents, BAPTA-AM also directly inhibits I_{Kr}.

MATERIALS AND METHODS

Isolation of single canine ventricular myocytes

Adult mongrel dogs of either sex were anaesthetized with intramuscular injections of 10 mg/kg ketamine hydrochloride (Calypsol, Richter Gedeon, Hungary) + 1 mg/kg xylazine hydrochloride (Sedaxylan, Eurovet Animal Health BV, The Netherlands) according to protocols approved by the local ethical committee (license N° 18/2012/DEMAB) in line with the ethical standards laid down in the Declaration of Helsinki in 1964 and its later amendments. The hearts were quickly removed and placed in Tyrode solution containing (in mM) NaCl, 144; KCl, 5.6; $CaCl_2$, 2.5; $MgCl_2$, 1.2; HEPES, 5; and dextrose, 11; at pH = 7.4. Single myocytes were obtained by enzymatic dispersion using the segment perfusion technique, as described previously (22, 23). Briefly, a wedge-shaped section of the left ventricular wall supplied by the left anterior descending coronary artery was cannulated, dissected and perfused with oxygenized Tyrode solution. After removal of blood the perfusion was switched to a nominally Ca^{2+}-free Joklik solution (Minimum Essential Medium Eagle, Joklik Modification, Sigma-Aldrich Co., St. Louis, MO, USA) for 5 min. This was followed by 35 min perfusion with Joklik solution supplemented with 1 mg/ml collagenase (Type II. Worthington, Chemical Co.) and 0.2% bovine serum albumin (Fraction V., Sigma-Aldrich Co.) containing 50 μM Ca^{2+}. The full transmural section of the middle portion of the left ventricular wall was cut into small pieces and the cell suspension was washed with Joklik solution. These tissue chunks, however, contained dominantly myocytes of midmyocardial origin. After gradually restoring the normal external Ca^{2+} concentration, the cells were stored in Minimum Essential Medium Eagle (Sigma-Aldrich Co.) until use. Drugs were obtained from Sigma-Aldrich Co.

Recording of action potentials

All electrophysiological measurements were performed at 37°C as previously described (23). Rod-shaped viable cells showing clear striation were sedimented in a plexiglass chamber of 1 ml volume allowing continuous superfusion (at a rate of 2 ml/min) with Tyrode solution. Transmembrane potentials were recorded using 3 M KCl filled sharp glass microelectrodes having tip resistance between 20 and 40 MO. These electrodes were connected to the input of Multiclamp 700A or 700B amplifiers (Molecular Devices, Sunnyvale, CA, USA). The cells were paced through the recording electrode at a steady frequency of 1 Hz using 1 – 2 ms wide rectangular current pulses having amplitudes of 120% of the diastolic threshold. Since the cytosol was not dialyzed, time-dependent changes in action potential morphology were negligible for the period of our experimental protocol not lasting longer than 40 min. Action potentials were digitized at 200 kHz using Digidata 1332A or 1440A digitizers (Molecular Devices) and stored for later analysis. BAPTA-AM was dissolved in DMSO to yield 5 mM stock solutions, which was diluted into the bathing solution immediately before use.

Conventional voltage clamp

The cells were superfused at 37°C with a modified Tyrode solution supplemented with 1 μM nisoldipine and 1 μM HMR 1556 to prevent the contamination with L-type Ca^{2+} current (I_{Ca}) and the slow delayed rectifier K^+ current (I_{Ks}) respectively. The modified Tyrode solution contained (in mM): NaCl, 121; KCl, 4; $CaCl_2$, 1.3; $MgCl_2$, 1; HEPES, 10; $NaHCO_3$, 25; and glucose, 10; at pH = 7.35. The osmolarity of this solution was 298 – 303 mOsm. Suction pipettes, made of borosilicate glass, had tip resistances of 2 – 3 MO after filling with pipette solution, containing (in mM) K-aspartate 100, KCl 45, $MgCl_2$ 1, HEPES 5, BAPTA 10, K-ATP 3, at pH = 7.2. Membrane currents were recorded with Multiclamp 700A or 700B amplifier (Molecular Devices) using the whole cell configuration of the patch clamp technique. After establishing high (1 – 10 GO) resistance seal by gentle suction, the cell membrane beneath the tip of the electrode was disrupted by further suction or by applying 1.5 V electrical pulses for 1 ms. Outputs from the amplifier were digitized at 20 kHz under software control (pClamp 10.0, Molecular Devices). The I_{Kr} was activated by 500 ms long depolarizing pulses clamped to +40 mV, arising from the holding potential of –80 mV. This protocol was repeated at a frequency of 0.05 Hz. I_{Kr} was assessed as tail current amplitudes recorded following repolarization to –40 mV for 10 s. Currents were normalized to cell capacitance, determined in each cell using hyperpolarizations from +10 to –10 mV for 15 ms. Series resistance was typically 4 – 8 MO before compensation (usually 50 – 80%). Experiments were discarded when the series resistance was high or substantially increased during the measurement.

Action potential voltage clamp

After establishment of whole-cell configuration, action potentials were recorded in current clamp mode from the myocytes superfused with a modified Tyrode solution described in the ‘conventional voltage clamp’ section. In these experiments no ion channel blocker was applied in the external solution in order to develop normal action potentials. The pipette solution contained (in mM): K-aspartate 130, KCl 30, MgATP 3, HEPES 10, Na_2-phosphocreatine 3, EGTA 0.01, cAMP 0.002, KOH 10, at pH = 7.3. As a consequence, the experimental conditions applied in action potential voltage clamp experiments were close to physiological (24, 25). The cells were continuously paced through the recording electrode at steady stimulation frequency of 1 Hz. A previously recorded ‘canonic’ canine midmyocardial action potential was applied to the voltage clamped cells as command voltage. Current traces were recorded continuously under ‘reference’ conditions (in the absence or presence of BAPTA-AM in the bathing medium) and after the application of the specific I_{Kr} inhibitor E 4031. I_{Kr} was defined as an E 4031-sensitive current obtained by subtracting the traces obtained in the presence of E 4031 from the ‘reference’ traces. To diminish the consequences of trace-to-trace fluctuations and to reduce noise, 20 consecutive I_{Kr} traces were averaged, and the averaged curve was used for further analysis.

In these experiments, to rule out the changes in current traces caused by the continuous calcium chelating effect of BAPTA-AM, cells were pre-loaded with BAPTA-AM before the measurements. To achieve this, cells were incubated with 5 μM BAPTA-AM for 20 min, then washed twice with Tyrode solution, and stored for at least further 15 minutes in BAPTA-AM-free Tyrode. These BAPTA-AM loaded cells, which did not contract when stimulated through the pipette, were used as control. To test the acute effect of BAPTA-AM on I_{Kr} in another group of cells, the superfusate was supplemented with 5 μM BAPTA-AM. In both cases I_{Kr} was identified as E 4031-sensitive current.

Statistical analysis

Results are expressed as mean ± SEM values. Statistical significance of differences from control was evaluated using one-way ANOVA followed by Student’s t-test for paired or unpaired data as pertinent. Differences were considered significant when P was less than 0.05.

RESULTS

Effect of BAPTA-AM on action potential morphology

The most conventional way to study the effect of changes in $[Ca^{2+}]_i$ on action potential configuration is loading the cell interior with the Ca^{2+} chelator BAPTA using its cell-permeant acetoxy-methylester form, or alternatively, to load the cells with Ca^{2+} using the Ca^{2+}-ionophore A23187. As presented in *Fig. 1*, exposure to 5 μM BAPTA-AM lengthened, while to A23187 shortened the duration of action potentials measured at 90% level of repolarization (APD_{90}). These changes developed gradually in a time-dependent manner (*Fig. 1C*) although in the case of BAPTA-AM there was an initial rapid rise in APD_{90}. Actions of BAPTA-AM and A23187 failed to fully saturate within the recording period of 30 min, probably due to the progressive intracellular accumulation of free BAPTA resulting in a more and more effective buffering of $[Ca^{2+}]_i$ in the first case and accumulation of Ca^{2+} in the second one. Furthermore, the changes in APD_{90} were accompanied with characteristic changes in action potential morphology, since reduction of $[Ca^{2+}]_i$ shifted the plateau potential to more positive voltages, while its elevation resulted in a marked depression of the plateau (*Fig. 1A* and *1B*).

The effect of BAPTA-AM was studied under conditions when the density of I_{Ca} was manipulated. In the presence of the Ca^{2+}-channel blocker nisoldipine (26) the BAPTA-AM-induced APD-lengthening was negligible (although statistically significant) and only transient since it disappeared after 20 min exposure to BAPTA-AM (*Fig. 2B* and *2D*). In contrast, increasing I_{Ca}-density with BAY K8644 (27) markedly augmented the BAPTA-AM-induced prolongation of APD_{90} (*Fig. 2C* and *2D*). It is worthy of note that BAPTA-AM showed a biphasic effect in the presence of BAY K8644. After 5 min exposure to BAPTA-AM APD_{90} reached its maximum, and after this it shortened gradually reaching a local minimum around 15 min of BAPTA-AM treatment (*Fig. 2C*).

The effects of nisoldipine and BAY K8644 on action potential configuration (plateau-depression by nisoldipine and elevation by BAY K8644) were qualitatively similar to those seen with A23189 and BAPTA-AM, respectively. Taken these findings, demonstrated in *Fig. 1* and *Fig. 2*, together, one might logically conclude that the reduction of $[Ca^{2+}]_i$ lengthens while its elevation shortens the action potential, furthermore, these effects are likely mediated *via* the Ca^{2+}-dependent inactivation of I_{Ca} (22).

Contrasting to the argumentation above, when the cells were pretreated with I_{Kr} blocker (100 nM dofetilide or 300 nM E 4031) BAPTA-AM shortened APD_{90} instead of lengthening it, as it is demonstrated in *Fig. 3C-3E*. The applied concentrations of I_{Kr} blockers eliminated more than 75% of I_{Kr} (28). This shortening effect, however, was temporary - strongly resembling the transient APD_{90}-shortening tendency observed with BAPTA-AM in the presence of BAY K8644 following the immediate APD_{90} lengthening effect of the former. On the other hand, the APD_{90}-lengthening effect of 100 nM dofetilide was significantly reduced in the presence of 5 μM BAPTA-AM (*Fig. 3F*). The effect of BAPTA-AM on action potential morphology was sensitive exclusively to the density of I_{Kr}, since blocking I_{Ks} with 1 μM HMR 1556 (29) failed to alter the effect of BAPTA-AM on action potential duration (*Fig. 3B* and *3E*). The effects of 5 min pretreatment with nisoldipine, BAY K8644, dofetilide and E 4031 (drugs used before the exposure to BAPTA-AM in *Fig. 2* and *Fig. 3*) on APD_{90} were comparable in magnitude to the those observed after longer exposures, lasting for 20 - 30 min, as shown in *Fig. 4*. This is important because any change in APD_{90} recorded in the

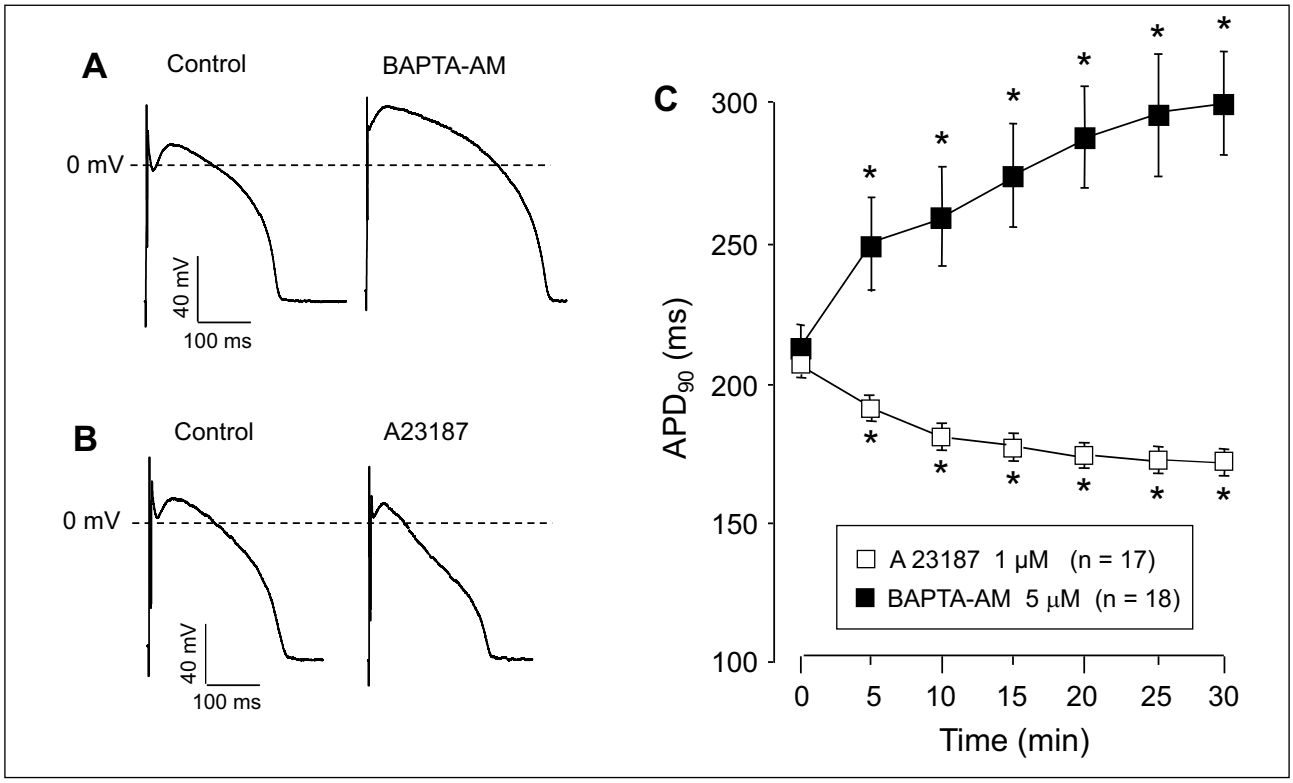

Fig. 1. Effects of changes in $[Ca^{2+}]_i$ on action potential duration (APD_{90}). (A), (B): Pairs of representative action potentials recorded from myocytes exposed to 5 μM BAPTA-AM (A) and 1 μM A23187 for 30 min (B). Time-dependent changes in APD_{90} are presented in panel (C). Symbols and bars are means ± SEM, asterisks indicate significant changes from the pre-drug control values. Numbers in parentheses indicate the number of myocytes studied.

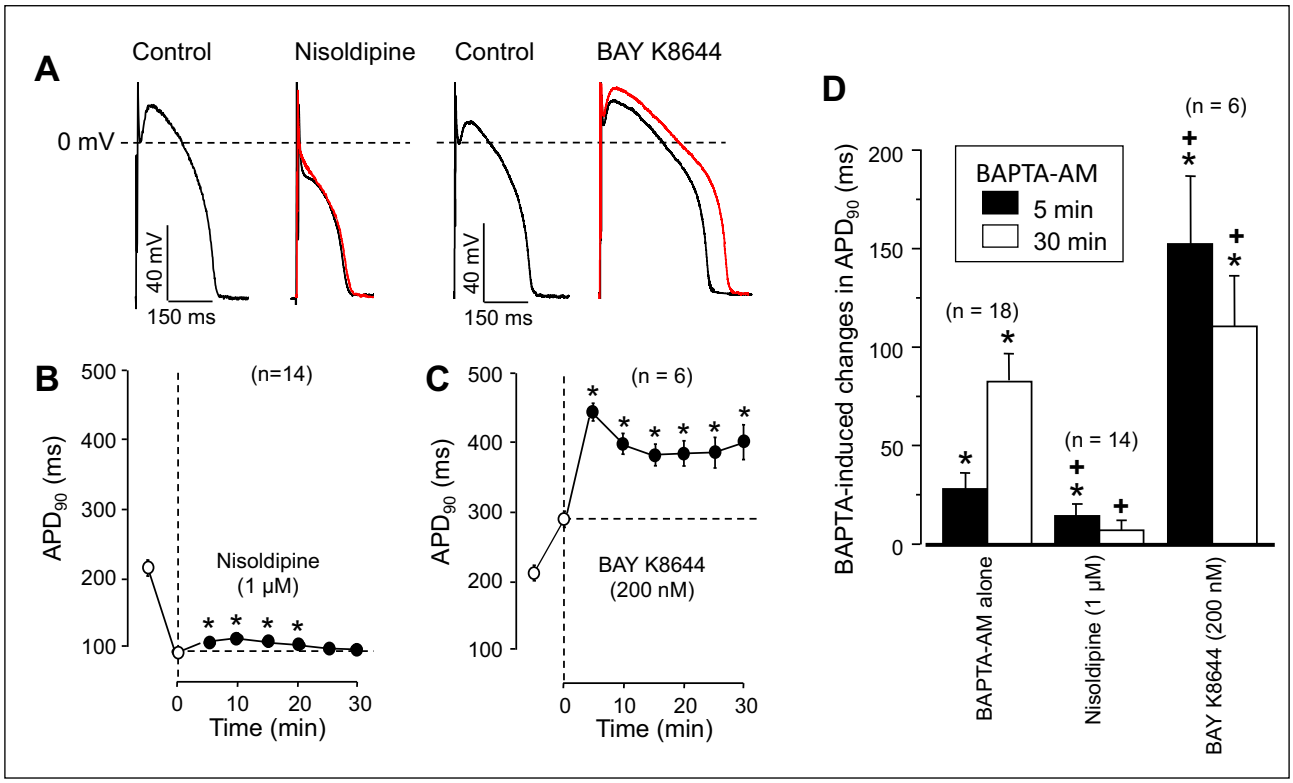

Fig. 2. Time-dependent effects of BAPTA-AM on action potential duration in the presence of nisoldipine and BAY K8644. (A): Representative analogue records showing the effects of 5 min exposure to nisoldipine and BAY K 8644 on action potential morphology (black records) Red records indicate superimposed action potentials obtained after 30 min superfusion with BAPTA-AM (in the continuous presence of nisoldipine or BAY K8644). (B), (C): Time-dependent effects of 5 μM BAPTA-AM in the presence of 1 μM nisoldipine (B) and 200 nM BAY K8644 (C) on APD90. Open symbols represent data obtained before the exposure to BAPTA-AM (first symbol: control; second symbol: after 5 min pretreatment with nisoldipine or BAY K8644), filled symbols show data recorded following superfusion with BAPTA-AM in the presence of nisoldipine or BAY K 8644. APD_{90} values measured at 5 and 30 min of BAPTA-AM are presented in panel (D). Symbols, columns and bars are arithmetic means ± SEM, asterisks denote significant differences from pre-BAPTA-AM (control) values, while crosses refer to significant changes comparing to the 'BAPTA-AM alone' group (data from *Fig. 1C*). Numbers in parentheses indicate the number of myocytes studied.

presence of BAPTA-AM cannot be attributed to time-dependent progression of the effect of the drug used for pretreatment.

To demonstrate that not BAPTA - but only BAPTA-AM - is responsible for the observed alterations in action potential morphology, myocytes were superfused with 5 μM BAPTA. No change in action potential duration or in other parameters were observed after 30 min exposure to BAPTA. (*Fig. 5A* and *5B*) indicating that the presence of the acetoxy-methyl group in the molecule is essential for the development of acute APD-lengthening effect of BAPTA-AM. The stability of our action potentials are documented in *Fig. 5C* and *5D*. Both the duration as well as the configuration of action potentials failed to alter significantly in untreated canine ventricular cells within the 60 min period of recording.

Effect of BAPTA-AM on I_{Kr} current

In the first set of experiments, the effect of externally applied BAPTA-AM was studied on I_{Kr} in 5 ventricular myocytes using the conventional patch clamp technique. The density of I_{Kr} was evaluated by the amplitude of I_{Kr} tail currents recorded upon repolarization to –40 mV. As indicated by *Fig. 6*, exposure of the cells to 5 μM BAPTA-AM for 5 min decreased the density of I_{Kr} to 32 ± 8 % of the control (from 0.39 ± 0.05 to 0.12 ± 0.03 A/F, $P < 0.05$, n = 5) in a partially reversible manner, since the current amplitude returned to 76 ± 5% of its control value during a 5 min period of washout with BAPTA-AM-free superfusate. As the pipette solution contained 10 mM BAPTA in these experiments, suppression of I_{Kr} by BAPTA-AM was independent of intracellular Ca^{2+} buffering.

Conventional voltage clamp experiments are not ideal to visualize the consequences of an ion current blockade during the action potential. Therefore action potential voltage clamp experiments have been designed to monitor the changes in I_{Kr} current profile following superfusion with 5 μM BAPTA-AM (*Fig. 7*). Since this technique is based on pharmacological extraction of I_{Kr} (using 1 μM E 4031), measurements had to be performed in two populations of myocytes. The density of I_{Kr} measured in the absence (control) and presence of external BAPTA-AM was 0.50 ± 0.03 and 0.17 ± 0.06 A/F (n = 7 and n = 5, respectively, $P < 0.05$), corresponding to a reduction of 66%. There was a similar difference in the amount of charge carried by I_{Kr} during the action potential: 22 ± 5 versus 6 ± 2 mC/F (n = 7 and n = 5, respectively, $P < 0.05$), a reduction to 27% of the control value. The Ca^{2+}-buffering effect of BAPTA-AM could be excluded in these experiments as well, because the cells had been pre-loaded with BAPTA before their exposure to external BAPTA-AM (see the Methods section for details).

DISCUSSION

In the present study, we have clearly shown that the frequently used Ca^{2+} chelator BAPTA-AM effectively and

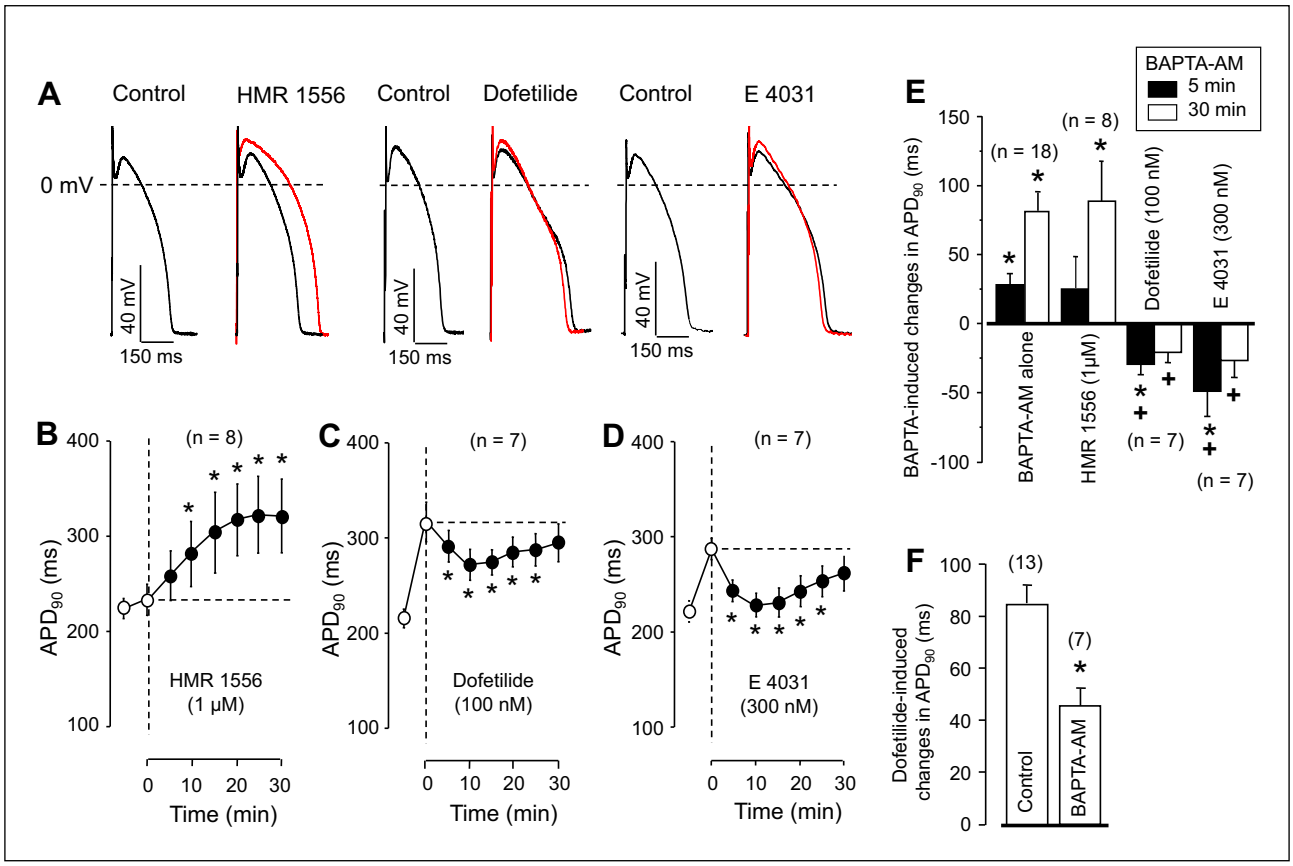

Fig. 3. Time-dependent effects of BAPTA-AM on action potential duration in the presence of different delayed rectifier potassium current blockers. (A): Effects of 5 min exposure to 1 μM HMR 1556, 100 nM dofetilide and 300 nM E 4031 on action potential configuration (black records). Action potentials taken following 30 min BAPTA-AM superfusion (in the continuous presence of HMR 1556, dofetilide or E 4031) are shown in red color. Panels (B) – D) indicate average data obtained with the I_{Ks}-blocker HMR 1556 (B), the I_{Kr} blocker dofetilide (C) or E-4031 (D). Open symbols represent data measured before the exposure to BAPTA-AM (first symbol: control; second symbol: 5 min pretreatment with HMR 1556, dofetilide or E 4031), filled symbols show data after superfusion with BAPTA-AM in the presence of HMR 1556, dofetilide or E 4031. (E): Changes in APD_{90} values observed at 5 and 30 min of BAPTA-AM treatment after pretreatment with various K^+ channel blockers. (F): APD-lengthening effect of 100 nM dofetilide alone and in the presence of 5 μM BAPTA-AM. Symbols, columns and bars are arithmetic means ± SEM, asterisks denote significant differences from pre-BAPTA-AM (control) values, while crosses refer to significant changes comparing to the 'BAPTA-AM alone' group. Numbers in parentheses indicate the number of myocytes studied. In panel (F), the asterisk denotes significant difference obtained in the absence and presence of BAPTA-AM.

reversibly blocked I_{Kr} in canine ventricular myocytes. Our results are in an excellent agreement with the results of Tang *et al*. (18), who reported an IC_{50} value of 1.3 μM for BAPTA-AM on hERG channels (and similar values for other K^+ channels) expressed in HEK 293 cells. These authors also reported an open channel block with BAPTA-AM. Therefore it is somewhat surprising that a similar degree of block was observed under conventional and action potential voltage clamp conditions (reduction to 32 and 34% of the control values, respectively). Probably the consequences of the more positive activation voltage of +40 mV, applied in conventional voltage clamp, compared to the less positive action potential plateau in action potential voltage clamp experiments, was offset by the higher stimulation frequency of 1 Hz used in the latter experimental design. The most important message of both voltage clamp experiments is that external BAPTA-AM must not be used as an experimental Ca^{2+} chelator when studying the Ca^{2+} dependence of cardiac ion currents in whole cell systems expressing hERG channels, because of the direct inhibitory effect of BAPTA-AM on I_{Kr} current.

Based on the present results, the exposure to BAPTA-AM displays a very complex pattern of changes in APD_{90}, so explanation of the results is necessarily speculative. The rapidly developing acute effect of BAPTA-AM, the significant prolongation of APD_{90}, is very likely due to the BAPTA-AM-induced inhibition of I_{Kr}, an effect evident within the initial 5 min of exposure. This explanation apparently contradicts to the finding that the acute lengthening effect of BAPTA-AM was reduced by nisoldipine and augmented by BAY K8644, which might suggest some kind of involvement of I_{Ca} in the concomitant changes of APD_{90}. However, not only I_{Ca} was increased or suppressed by BAY K8644 and nisoldopine, respectively, but also the pre-BAPTA value of APD_{90} as well as the level of the plateau potential. Consequences of the I_{Kr}-blockade strongly increases when APD_{90} is longer (30, 31), as was the case in the presence of BAY K8644, and decreases if APD_{90} is shorter, as was observed in the presence of nisoldipine. In addition, the relative importance of I_{Kr} in regulation of APD_{90} strongly increases with positive shifts in the plateau potential due to the faster activation of I_{Kr} at more positive voltages (28). This may also contribute to the stronger BAPTA-AM-induced prolongation in the presence of BAY K8644 versus the smaller change observed in nisoldipine.

When the I_{Kr}-blocking effect of BAPTA-AM was prevented by pretreatment of the cells with I_{Kr} blocking drugs, like

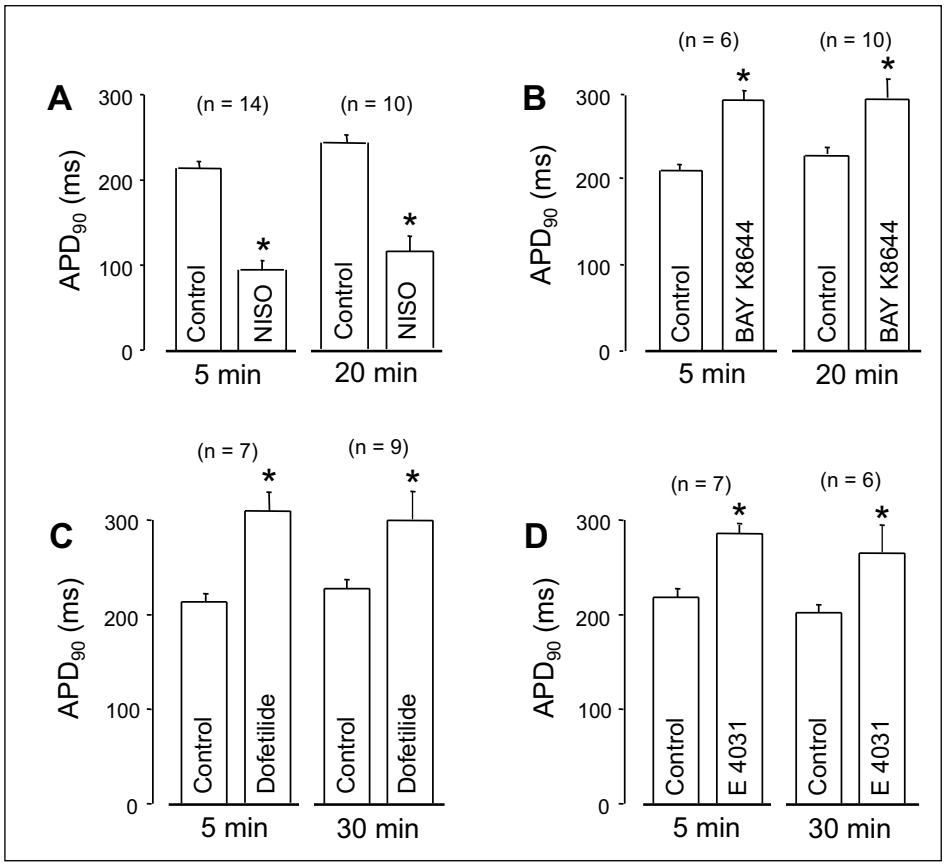

Fig. 4. Comparison of short term and long term effects of 1 μM nisoldipine (A), 200 nM BAY K8644 (B), 100 nM dofetilide (C) and 300 nM E 4031 (D) on APD_{90} in canine ventricular myocytes. Short term (5 min) and long term (20 – 30 min) effects were studied in different experiments. Columns and bars are arithmetic means ± SEM, asterisks denote significant differences from control values, and numbers in parentheses indicate the number of myocytes studied. No significant differences were observed between the long term and short term effects of the studied agents.

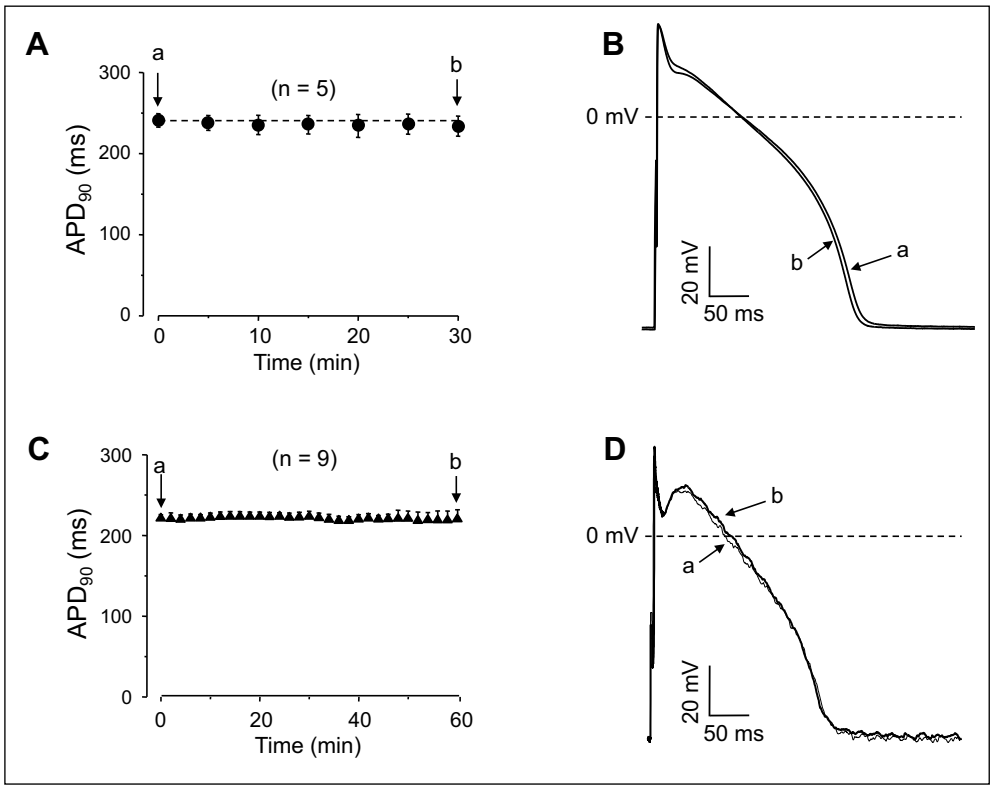

Fig. 5. Lack of effect of 5 μM externally applied BAPTA on action potential duration (A) and action potential configuration (B). Stability of action potential duration (C) and action potential morphology (D) in untreated cardiomyocytes. Superimposed action potentials, recorded from the same cell at the beginning (a) and the end (b) of the recording period are presented in panels (B) and (D). Symbols and bars represent mean ± SEM values, numbers in parentheses indicate the number of myocytes studied.

dofetilide or E 4031, BAPTA-AM initially shortened APD_{90}, an effect likely related to the reduction of $[Ca^{2+}]_i$. The most plausible explanation for this BAPTA-AM-induced shortening is the conversion of the normally inwardly directed Na^+/Ca^{2+} exchange (NCX) current to an outwardly directed one as a consequence of the reduced $[Ca^{2+}]_i$. In line with this, the tendency of APD-shortening observed after the initial BAPTA-AM-induced prolongation in myocytes pretreated with BAY

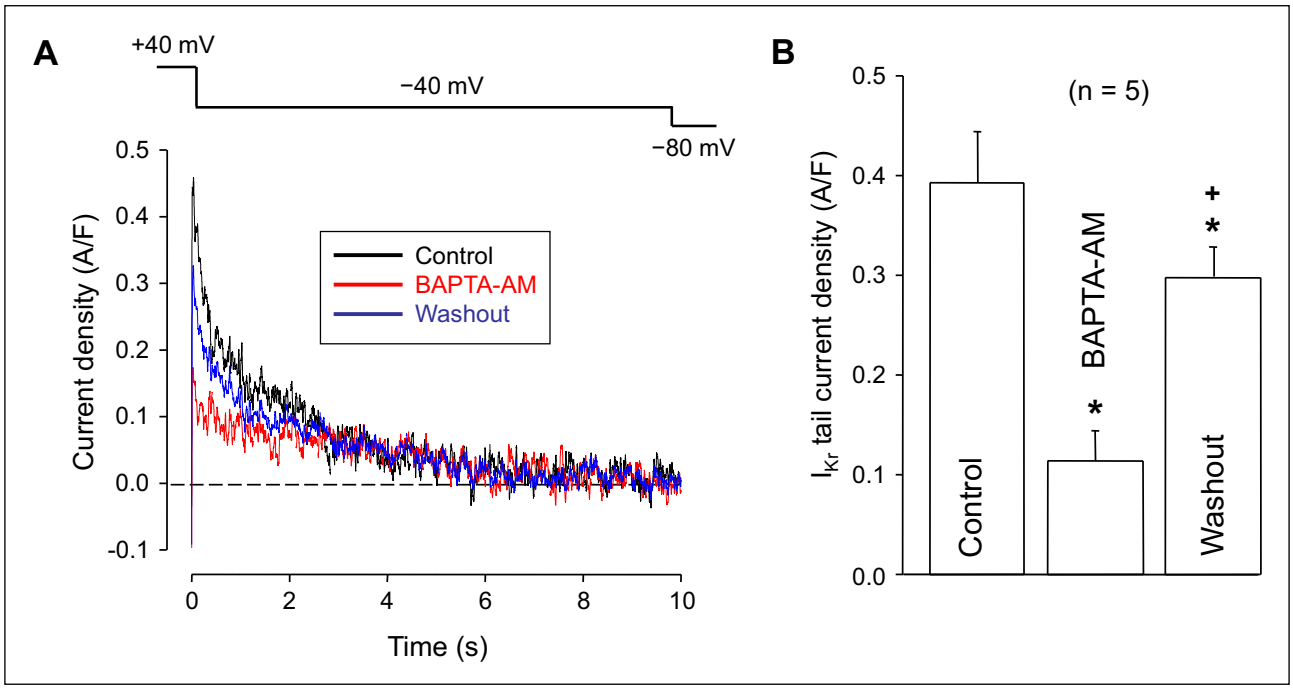

Fig. 6. Effect of BAPTA-AM on I_{Kr} under conventional voltage clamp conditions. (A): Representative set of superimposed I_{Kr} tail current traces recorded following repolarization to –40 mV. The current was activated at +40 mV for 500 ms as shown by the applied voltage protocol (above). The cell was exposed to 5 µM BAPTA-AM for 5 min, which was followed by a subsequent 5 min period of washout. (B): Average I_{Kr} tail current amplitudes measured before (control) in the presence of, and after the washout of BAPTA-AM. Columns and bars are arithmetic means ± SEM, asterisks denote significant differences from control, the cross refers to significant changes upon washout of BAPTA-AM, and the number in parentheses indicates the number of myocytes studied.

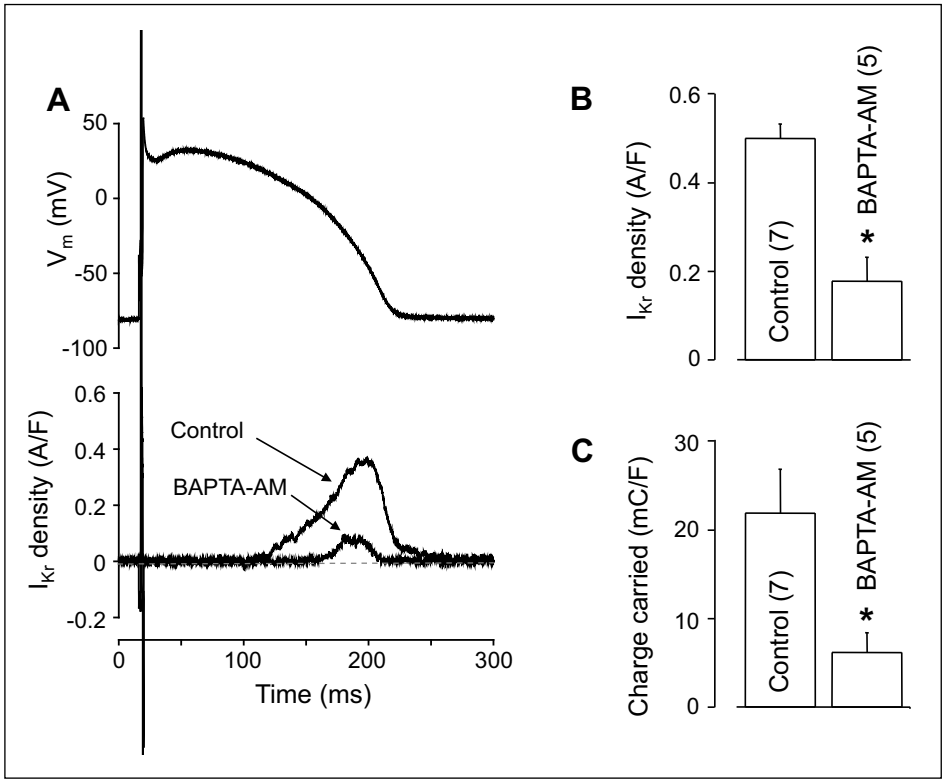

Fig. 7. Effect of BAPTA-AM on I_{Kr} under action potential voltage clamp conditions. (A): The command action potential (above) and representative superimposed I_{Kr} current traces recorded in the absence (control) and presence of 5 µM BAPTA-AM applied in the superfusate for 5 min. Both groups of cells were pre-loaded with BAPTA-AM for 20 min in order to load the cells with BAPTA before the measurements. (B) and (C): Peak amplitude of I_{Kr} and the total change carried by the current, respectively, measured in absence and presence of extracellular BAPTA-AM. Columns and bars are arithmetic means ± SEM, asterisks denote significant differences between the groups of cells exposed - or not exposed - to extracellular BAPTA-AM. Numbers in parentheses indicate the number of myocytes studied.

K8644 was also pronounced probably because the long APD_{90} and the positive plateau potential favored the reverse mode activity of NCX (32, 33). This effect is in line with the finding that buffering $[Ca^{2+}]_i$ significantly shortened APD_{90} in rat, guinea pig and ferret cardiomyocytes (34, 35) and with own unpublished results, obtained in guinea pig ventricular cells, indicating that net NCX current was outward when recorded with EGTA-containing patch pipettes.

As documented in *Figs*. *3C* and *3D*, the BAPTA-AM-induced APD_{90}-shortening effect was transient. In other words, there was a progressive tendency of prolongation during a long-lasting exposure to BAPTA-AM. This was also evident under control conditions, where no transient shortening was observed (only a small notch after 5 min). The final lengthening tendency of APD_{90} is likely related to the combination of two further effects of progressive buffering of $[Ca^{2+}]_i$. These are the augmentation of the I_{Ca} due to the reduction of its Ca^{2+}-dependent inactivation (22) and offsetting some Ca^{2+}-dependent outward currents, like the Ca^{2+}-dependent Cl^- current by buffering $[Ca^{2+}]_i$ (7, 8). In summary, buffering of $[Ca^{2+}]_i$ resulted in a biphasic response of APD_{90}: a transient initial shortening was followed by progressive prolongation when the I_{Kr}-blocking effect of BAPTA-AM was prevented by the pretreatment with dofetilide or E 4031.

Acknowledgements: This work was funded by the National Research Development and Innovation Office (NKFIH-K115397, NKFIH-K109736, NKFIH-PD120794 and OTKA: ANN-113273). Support was obtained from GINOP-2.3.2.-15-2016-00040 and EFOP-3.6.2-16-2017-00006 projects, which are co-financed by the European Union and the European Regional Development Fund. Further support was provided by the Janos Bolyai Research Scholarship of the Hungarian Academy of Sciences (to NS and BH) and the University of Debrecen (RH/751/2015) to NS. The work was also supported by the UNKP-17-4-III-DE-201 New National Excellence Program of the Ministry of Human Capacities. The authors thank Miss Eva Sagi for excellent technical assistance.

B. Horvath and N. Szentandrassy have equally contributed to this study.

Conflict of interests: None declared.

REFERENCES

1. Tan HL, Kupershmidt S, Zhang R, *et al*. A calcium sensor in the sodium channel modulates cardiac excitability *Nature* 2002; 415: 442-447.
2. Mori M, Konno T, Ozawa T, Murata M, Imoto K, Nagayama K. Novel interaction of the voltage-dependent sodium channel (VDSC) with calmodulin: does VDSC acquire calmodulin-mediated Ca^{2+}-sensitivity? *Biochemistry* 2000; 39: 1316-1323.
3. Lee A, Wong ST, Gallagher D, *et al*. Ca^{2+}/calmodulin binds to and modulates P/Q-type calcium channels. *Nature* 1999; 399: 155-159.
4. DeMaria CD, Soong TW, Alseikhan BA, Alvania RS, Yue DT. Calmodulin bifurcates the local Ca^{2+} signal that modulates P/Q-type Ca^{2+} channels. *Nature* 2001; 411: 484-489.
5. Tuteja D, Xu D, Timofeyev V, *et al*. Differential expression of small-conductance Ca^{2+}-activated K^+ channels. SK1, SK2, and SK3 in mouse atrial and ventricular myocytes. *Am J Physiol Heart Circ Physiol* 2005; 289: H2714-H2723.
6. Nattel S, Qi XY. Calcium-dependent potassium channels in the heart: clarity and confusion. *Cardiovasc Res* 2014; 101: 185-186.
7. Horvath B, Vaczi K, Hegyi B, *et al*. Sarcolemmal Ca^{2+}-entry through L-type Ca^{2+} channels controls the profile of Ca^{2+}-activated Cl^- current in canine ventricular myocytes. *J Mol Cell Cardiol* 2016; 97: 125-139.
8. Hegyi B, Horvath B, Vaczi K, *et al*. Ca^{2+}-activated Cl^- current is antiarrhythmic by reducing both spatial and temporal heterogeneity of cardiac repolarization. *J Mol Cell Cardiol* 2017; 109: 27-37.
9. Weber CR, Piacentino V, Ginsburg KS, Houser SR, Bers DM. Na^+-Ca^{2+} exchange current and submembrane $[Ca^{2+}]$ during the cardiac action potential. *Circ Res* 2002; 90: 182-189.
10. Quednau BD, Nicoll DA, Philipson KD. Tissue specificity and alternative splicing of the Na^+/Ca^{2+} exchanger isoforms NCX1, NCX2, and NCX3 in rat. *Am J Physiol* 1997; 272: C1250-C1261.
11. Guinamard R, Chatelier A, Demion M, *et al.* Functional characterization of a Ca^{2+}-activated non-selective cation channel in human atrial cardiomyocytes. *J Physiol* (*Lond*) 2004; 558: 75-83.
12. Guinamard R, Bouvagnet P, Hof T, Liu H, Simard C, Salle L. TRPM4 in cardiac electrical activity. *Cardiovasc Res* 2015; 108: 21-30.
13. Billman GE, McIlroy B, Johnson JD. Elevated myocardial calcium and its role in sudden cardiac death. *FASEB J* 1991; 5: 2586-2592.
14. Billman GE. Intracellular calcium chelator, BAPTA-AM, prevents cocaine-induced ventricular fibrillation. *Am J Physiol Heart Circ Physiol* 1993; 265: H1529-H1535.
15. Warren M, Huizar JF, Shvedko AG, Zaitsev AV. Spatiotemporal relationship between intracellular Ca^{2+} dynamics and wave fragmentation during ventricular fibrillation in isolated blood-perfused pig hearts. *Circ Res* 2007; 101: e90-e101.
16. Ogawa M, Lin SF, Weiss JN, Chen PS. Calcium dynamics and ventricular fibrillation. *Circ Res* 2008; 102: e52. doi: 10.1161/CIRCRESAHA.108.171538
17. Younes A, Lyashkov AE, Graham D, *et al*. Ca^{2+}-stimulated basal adenylyl cyclase activity localization in membrane lipid microdomains of cardiac sinoatrial nodal pacemaker cells. *J Biol Chem* 2008; 283: 14461-14468.
18. Tang Q, Jin MW, Xiang JZ, *et al*. The membrane permeable calcium chelator BAPTA-AM directly blocks human ether a-go-go-related gene potassium channels stably expressed in HEK 293 cells. *Biochem Pharmacol* 2007; 74: 1596-1607.
19. Szentandrassy N, Papp F, Hegyi B, Krasznai Z, Nanasi PP. Tetrodotoxin blocks native cardiac L-type Ca^{2+} channels but not $Ca_v1.2$ channels expressed in HEK cells. *J Physiol Pharmacol* 2013; 64: 807-810.
20. Szabo G, Szentandrassy N, Biro T, *et al*. Asymmetrical distribution of ion channels in canine and human left ventricular wall: epicardium versus midmyocardium. *Pflugers Arch* 2005; 450: 307-316.
21. Szentandrassy N, Banyasz T, Biro T, *et al*. Apico-basal inhomogeneity in distribution of ion channels in canine and human ventricular myocardium. *Cardiovasc Res* 2005; 65: 851-860.
22. Kistamas K, Szentandrassy N, Hegyi B, *et al*. Changes in intracellular calcium concentration influence beat-to-beat variability of action potential duration in canine ventricular myocytes. *J Physiol Pharmacol* 2015; 66: 73-81.
23. Szentandrassy N, Horvath B, Vaczi K, *et al*. Dose-dependent electrophysiological effects of the myosin activator omecamtiv mecarbil in canine ventricular cardiomyocytes. *J Physiol Pharmacol* 2016; 67: 483-489.
24. Chen-Izu Y, Izu LT, Nanasi PP, Banyasz T. From action potential-clamp to 'onion-peeling' technique - recording of ionic currents under physiological conditions. In: Patch Clamp Technique, Kaneez FS (ed). InTech 2012, 143-162.
25. Chen-Izu Y, Izu LT, Hegyi B, Banyasz T. Recording of ionic currents under physiological conditions: action potential-clamp and 'onion-peeling' techniques. In: Modern Tools of Biophysics, Jue T. (ed). Springer 2017; 31-48.

26. Sanguinetti MC, Kass RS. Voltage-dependent block of calcium channel current in the calf cardiac Purkinje fiber by dihydropyridine calcium channel antagonists. *Circ Res* 1984; 55: 336-348.
27. Sanguinetti MC, Krafte DS, Kass RS. Voltage-dependent modulation of Ca^{++} channel current in heart cells by BAY K8644. *J Gen Physiol* 1986; 88: 369-392.
28. Jurkiewicz NK, Sanguinetti MC. Rate-dependent prolongation of cardiac action potentials by a methanesulfonanilide class III antiarrhythmic agent specific block of rapidly activating delayed rectifier K^+ current by dofetilide. *Circ Res* 1993; 72: 75-83.
29. Thomas GP, Gerlach U, Antzelevitch C. HMR 1556, a potent and selective blocker of slowly activating delayed rectifier potassium current. *J Cardiovasc Pharmacol* 2003; 41: 140-147.
30. Banyasz T, Horvath B, Virag L, *et al*. Reverse rate dependency is an intrinsic property of canine cardiac preparations. *Cardiovasc Res* 2009; 84: 237-244.
31. Barandi L, Virag L, Jost N, *et al*. Reverse rate-dependent changes are determined by baseline action potential duration in mammalian and human ventricular preparations. *Basic Res Cardiol* 2010; 105: 315-323.
32. Ginsburg KS, Weber CR, Bers DM. Cardiac Na^+Ca^{2+}exchanger: dynamics of Ca^{2+}-dependent activation and deactivation in intact myocytes. *J Physiol* (*Lond*) 2013; 591: 2067-2086.
33. Birinyi P, Toth A, Jona I, *et al*. The Na^+/Ca^{2+} exchange blocker SEA0400 fails to enhance cytosolic Ca^{2+} transient and contractility in canine ventricular cardiomyocytes. *Cardiovasc Res* 2008; 78: 476-484.
34. Janvier NC, Mcmorn SO, Harrison SM, Taggart P, Boyett MR. The role of inward Na^+/Ca^{2+} exchange current in electrical restitution in ferret ventricular cells. *J Physiol* (*Lond*) 1997; 504: 301-314.
35. Mitchell M, Powell T, Terrar DA, Twist VW. The effects of ryanodine, EGTA and low-sodium on action potentials in rat and guinea-pig ventricular myocytes: evidence for two inward currents during the plateau. *Br J Pharmacol* 1984; 81: 543-550.

Received: January 2, 2018
Accepted: February 26, 2018

Author's address: Prof. Peter P. Nanasi, Department of Physiology and Department of Dental Physiology and Pharmacology, University of Debrecen, H-4012 Debrecen, P.O.Box 22, Hungary.
E-mail: nanasi.peter@med.unideb.hu